scientific reports

Check for updates

OPEN

Novel inhibitor against Rac1 for therapeutic approach in prevention of breast cancer progression

Abhinay Kunar Singh[1], Tirthankar Koley[1], Deepak Vats[2], Archana Singh[2], Ethayathulla Abdul Samath[1], Atul Batra[3] & Sharmistha Dey[1]✉

Metastatic breast-cancer is one of the major causes of death, due to remaining dormant cancer cells for several years. Rac1 is upregulated with cancer and stay elevated throughout the metastatic pathway to regulate the formation of lamellipodia and filopodia. This work developed peptide FGDWS as novel inhibitor targeting Rac1-Tiam1 binding site by in-silico as it was found to be the strongest interacting peptide with Rac1 at the Tiam binding site. The binding and inhibition study of peptide with Rac1 was performed by Surface plasmon resonance and MTT assay, respectively. Cell-migration, apoptotic assay and western-blot in breast-cancer cells were performed with FGDWS and in combination with Doxorubicin (Dox). Tumor regression experiment was done with mice model. The strong binding of FGDWS with Rac1 and reduction of cell-viability were observed in breast-cancer cell-lines. The cell-migration was suppressed, and higher regression were obtained in synergy group. The apoptotic effect of FGDWS alone and with Dox were detected by annexin-V via activating caspase3/7. The tumor size was reduced by the treatment of FGDWS and more reduced in combinatorial effect. The combinatorial effect of FGDWS-Dox may enhance the treatment efficacy without side-effects.

Keywords Breast cancer, Inhibitor, apoptosis, Rac1, Metastasis, Tumor

Abbreviations

Dox	Doxorubicin
Tiam1	T cell lymphoma invasion and metastasis 1
RMSD	Root mean square deviation
RMSF	Root mean square fluctuation
Rg	Radious of gyration
DMF	N, N-dimethylformamide
NMM	N-methylmorpholine
HBTU	O-(Benzotriazol-1-yl)-N,N,N′,N′-tetramethyluronium hexafluorophosphate
TFA	Trifluoroacetic acid
SPR	Surface plasmon resonance
EDC	N-ethyl- N'-3diethylaminopropylcarbodiimide
NHS	N-hydroxysuccinimide
KA	Association constant
KD	Dissociation constant
DMEM	Dulbaco modified minimum essential media
MTT	3-(4,5-dimethylthiazol-2-yl)-2,5-diphenyltetrazolium bromide
CT	Control
VC	Vehicle control
DMSO	Dimethylsulfoxide
PI	Propidium iodide
VEGF	Vascular endothelial growth factor
HC	Healthy control
TC	Tumor control
EAC	Ehrlich ascites carcinoma

[1]Department of Biophysics, All India Institute of Medical Sciences, Ansari Nagar, New Delhi 110029, India. [2]Department of Biochemistry, All India Institute of Medical Sciences, New Delhi 110029, India. [3]Department of Medical Oncology, All India Institute of Medical Sciences, New Delhi 110029, India. ✉email: sharmistha_d@hotmail.com

RIPA	Radioimmunoprecipitation assay
RLU	Relative luminance unit
ROS	Reactive oxygen species
AUC	Area under curve
GEF	Guanine nucleotide exchange factors
EGFR	Epidermal growth factor receptor
PAKs	p21-activated kinases
MAPKs	Mitogen-activated protein kinases
VASP	Vasodilator stimulating phospho protein
ER	Oestrogen receptor
BCA	Bicinchoninic acid assay

Breast-cancer is the most prominent cancer in women globally. Recent rapid increase of breast-cancer is probably due to change of lifestyle, eating habits, obesity, smoking and unhealthy diet. Early diagnosis of metastasis breast-cancer is very challenging. The tumor cells remain dormant for many years and show no sign of development for a long period of time, then slowly the cells migration initiates and proceeds towards different organs and turns to metastasis breast-cancer. It is important to understand the molecular pathway which initiates and switches towards cell migration. In our previous study we have observed that some crucial proteins like Rac1, p38 MAPK, LIMK1 and Cofilin1 in the cytoskeletal pathways are involved in the metastasis, those are overexpressed in the serum level at early stage of metastasis breast-cancer[1]. Among those protein Rac1 is the key molecule regulator for cell morphological changes by regulating the formation of lamellipodia and filopodia. Rac1 is the cytoskeletal regulator which promotes the migration of cells by polymerizing actin. One of the Rac1 pathway which is extensively studied in breast cancer metastasis, primarily activated by T-cell lymphoma invasion and metastasis-1 (Tiam1), which in turn phosphorylate and activate LIMK1 through p38α MAPK and further activate Cofilin1[2]. The hyperactivity and overexpression of Rac1 are well evidenced with aggressive growth and malignant tumor types[3]. Further, Rac1 also reduces multidrug resistance of breast-cancer cells to neoadjuvant chemotherapy as well as radiotherapy[4,5]. It is evidenced that inhibition of Rac1 activity can overcome the treatment resistance[6]. Targeting Rac1 can serve better for therapeutic agent in early breast-cancer stage. Small molecule inhibitors of Rac1 in the research stage are available in the literature: NSC23766 an inhibitor of Rac1 which induce G1 cell cycle arrest and apoptosis in breast-cancer cells[7] was reported first and it became the lead compound for designing small molecule against Rac1.

Current trend of pharmaceutical companies attracting the attention of developing peptide as drug due to several advantages. Peptide as a drug include their high specificity, potency, and activity. We demonstrated small peptide, FDGWS as an inhibitor of Rac1 targeting the NSC23766 binding site through downregulating the downstream molecules, p38MAPK, LIMK1 and Cofilin1 both in-vitro and in-vivo model. It prevented cell migration and induce apoptosis in breast-cancer cells and supressed the tumor size by inhibiting at the early stage of tumor in mice model.

Results

Molecular docking and MD simulations

The Fig. 1a represent the crystal structure of the Rac1-Tiam1 complex which was used to design peptide inhibitors against Rac1. The designed peptides showed binding energy in the range of -9 to -10 kcal/mol. The docking study showed that FGDWS formed 5 stable hydrogen-bonded interactions with Rac1 residues along with several hydrophobic interactions shown in (Fig. 1b). The peptide formed H-bonded interactions with Y64, D65, D38 and R66 of Rac1. The Ser of peptide formed a stable H-bond with D38 of Rac1. The Trp of the peptide was stacked between V36, W56 and L67 of Rac1, forming stable hydrophobic interactions. The peptide AVKYM formed 6 stable hydrogen-bonded interactions with Rac1 residues along with several hydrophobic interactions shown in (Fig. 1c). The peptide formed H-bonded interactions with V36, T35, V36, D65 and R66. The Lys of peptide formed a salt bridge with D38. The Met of the peptide was stacked between W56 and L67 forming stable hydrophobic interactions. The peptide GFKQC formed 6 stable hydrogen-bonded interactions with Rac1 residues along with several hydrophobic interactions shown in Fig. 1d. The peptide formed H-bonded interactions with T35, V36, D38, G60 and A69. The Ser of peptide formed a stable H-bond with D38. The Phe of the peptide was stacked between V36, W56 and L67 forming stable hydrophobic interactions.

After 100 ns MD simulations, the trajectory showed that the FGDWS was more stable compared to the other two peptides AVKYM, and GFKQC (Figure S1). The FGDWS was bound stable to the Tiam binding site of Rac1 with the Trp residue of the peptide buried deep inside the pocket. The peptide formed stable H-bonds with R66, D65 and E62 along with hydrophobic interactions with residues V36, W56, Y64, L67, R68, P69 and Y72 (Fig. 1e). The other two peptides moved out of the Tiam1 binding site. The cartoon representation shows that the peptide FGDWS binding to Rac1 prevents the Tiam1 binding (Fig. 1f).

The conformational stability of Rac1-peptide complexes was analysed after 100 ns Molecular Dynamics simulation performed using GROMACS. The overall RMSD of the Cα atoms of Rac1-peptide complexes were found to be in the range of 0.2 to 0.5 Å. The highest fluctuations were observed in the Rac1-AVKYM followed by FGDWS and GFKQC. The RMSF of the Cα backbone of the Rac1 was fluctuating in the range of 0.1 to 0.5 (Figure S2).

Binding assay of FGDWS with Rac1 by SPR

Recombinant Rac1 protein were immobilized successfully on CM5 sensor chip with 4000 RU, where 1 RU corresponds to 1pg/mm^2 (Figure S3). Different concentrations of FGDWS peptide passed on immobilized Rac1. The increased of RU with corresponding increase in concentration of peptide, showed the peptide specificity for

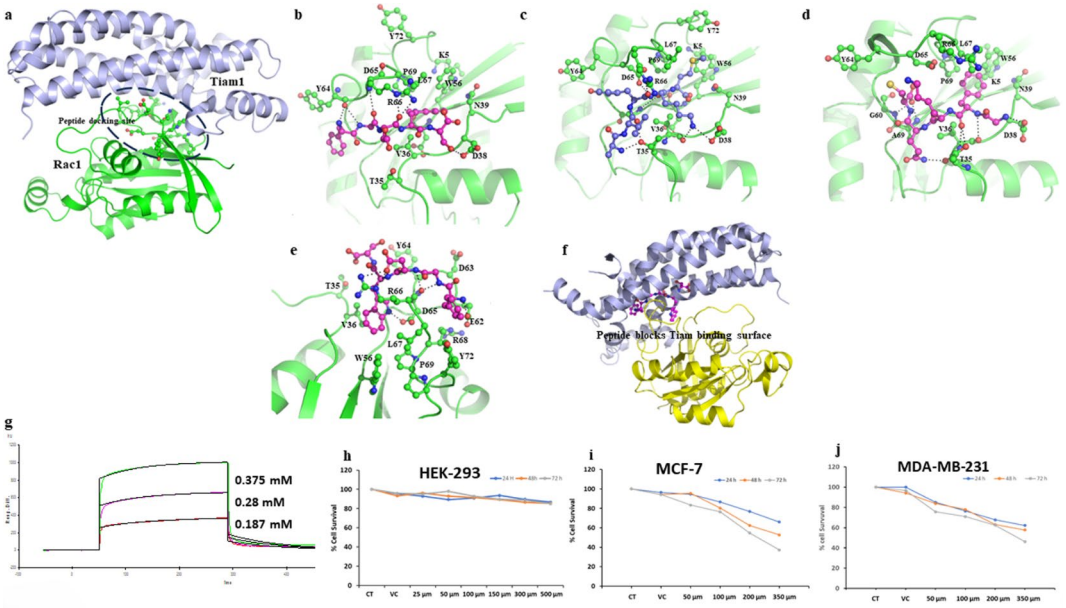

Fig. 1. Docking of designed peptide with Rac1-Tiam1 binding site, binding study of peptide with Rac1 and cytotoxicity assessment of peptide on HEK-293, MCF-7 and MDA-MB-231. (**a**) The cartoon representation of Rac1-Tiam1 complex (PDB ID: 1foe) along with Rac1 residues involved in interactions with Tiam1 shown in ball-in-stick. The H-bonded and non-polar interaction formed between the designed peptides (**b**) FGDWS, (**c**) AVKYM and (**d**) GFKQC. (**e**) The H-bonded and non-polar interactions formed by peptide FGDWS with Rac1 residues after 100 ns MD simulations. (**f**) The cartoon representation shows that the peptide FGDWS binding to Rac1 prevents the Tiam1 binding. (**g**) The binding study of FGDWS with Rac1 protein by SPR. (**h**–**j**) are graphs represent cytotoxicity assessments of FGDWS on HEK-293, MCF-7 and MDA-MB-231, respectively.

the protein (Fig. 1g). KA and KD value for the peptide binding with Rac1 were 1.24×10^6 M and 8.07×10^{-7} M, respectively, where higher KA demonstrate the faster binding of peptide with protein and lower KD represents the stronger binding.

Effect of peptide on cell lines

Cell viability assay

In MTT assay, FGDWS showed no toxic effect on normal HEK-293 cell line (Fig. 1h) whereas this peptide reduced the cell viability by 65–70% of MCF-7 and MDA-MB-231 cells, respectively (Fig. 1i & j). Cell viability of MCF-7 and MDA-MB-231 were found to be decreased in dose dependent manner with time.

Cell migration assay

The effect of peptide on cancer cell migration showed the cells were migrated and covers the scratched area of CT (Control) and VC (Vehicle control) group in both the breast cancer cell line MCF-7 (Fig. 2a) and MDA-MB-231 (Fig. 2b), whereas the rate of cell migration was slower with increase in concentration of peptide dose with time. The higher regression in migration were obtained in synergy group Dox + P3 (0.2 µm + 300 µm) at 48 and 72 h. The rate of cell proliferation and migration among all group in both the cell line were found to be slowest in Dox + P3 followed by Dox, P3, P2 and P1 after 48 h and 72 h of treatments. The bar diagram of percentage migration for both cell lines and cell migration figure of 4x resolution are illustrated in figure S4.

Apoptosis assay

Caspase glow 3/7 assay Caspase activity is directly proportional to RLU (relative luminance unit) and found to be increased significantly in both the cell lines MCF-7 ($p \leq 0.0001$) (Fig. 3a, b&c) and MDA-MB-231 ($p \leq 0.0001$) (Fig. 3d, e&f) in dose dependent manner. In MCF-7, the fold change in RLU in P1, P2, P3, Dox and Dox + P3 group with respect to control after 48 h were 0.24, 0.402, 0.93, 1.64 and 4.205, respectively and for MDA-MB-231 were 0.16, 0.25, 0.305, 0.84 and 1.104, respectively. After 72 h of treatments the fold change of RLU in MCF-7 cell line in P1, P2, P3, Dox and Dox + P3 group with respect to control were found to be 0.33, 0.47, 0.66, 0.79 and 1.49 respectively, whereas in case of MDA-MB-231 were 0.35, 0.57, 0.65, 1.02 and 1.53 respectively. No significant change in RLU was reported after 24 h in both the cell lines (Fig. 3a&d).

The comparison was also made between Dox + P3vs Dox and Dox + P3vs P3 groups. After 48 and 72 h treatment caspase activity was significantly ($p \leq 0.001$) high in Dox + P3 group than Dox alone, similarly Dox + P3 also showed significant ($p \leq 0.001$) upsurge in caspase activity than P3 alone for both the cell lines.

Annexin-V assay Apoptotic and necrotic cells were analysed based on the staining of cells with Annexin-V and PI (Propidium iodide), respectively. The phosphatidyl serine flips on outer side of plasma membrane at the

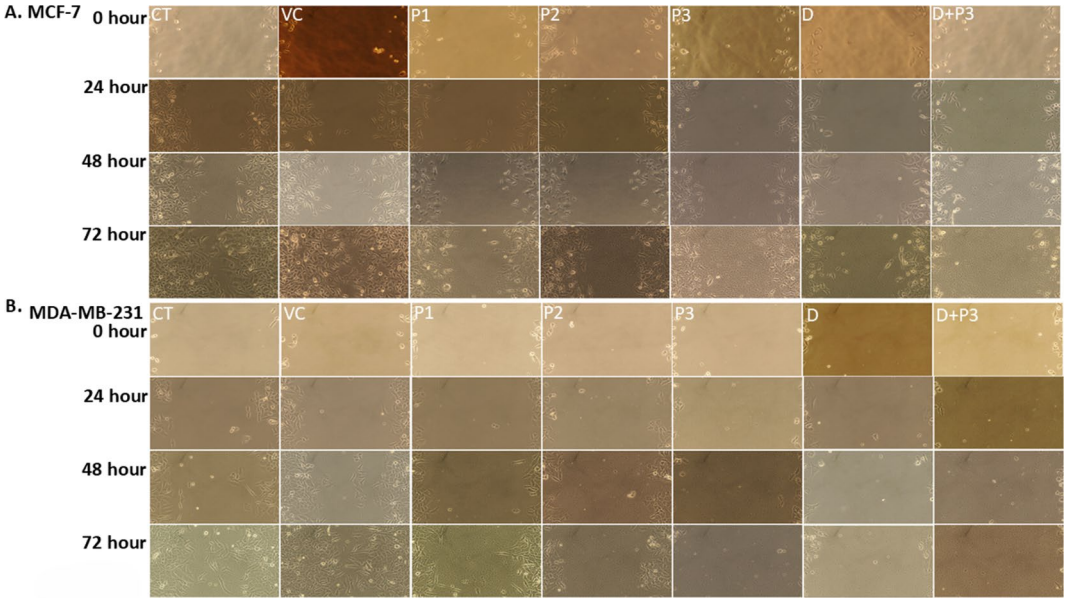

Fig. 2. Effect of FGDWS on Cell migration: Cell migration assay image of (**a**) MCF-7 and (**b**) MDA-MB-231 representing migration of cells in scratched area in different treatments group after 0, 24, 48 and 72 h.

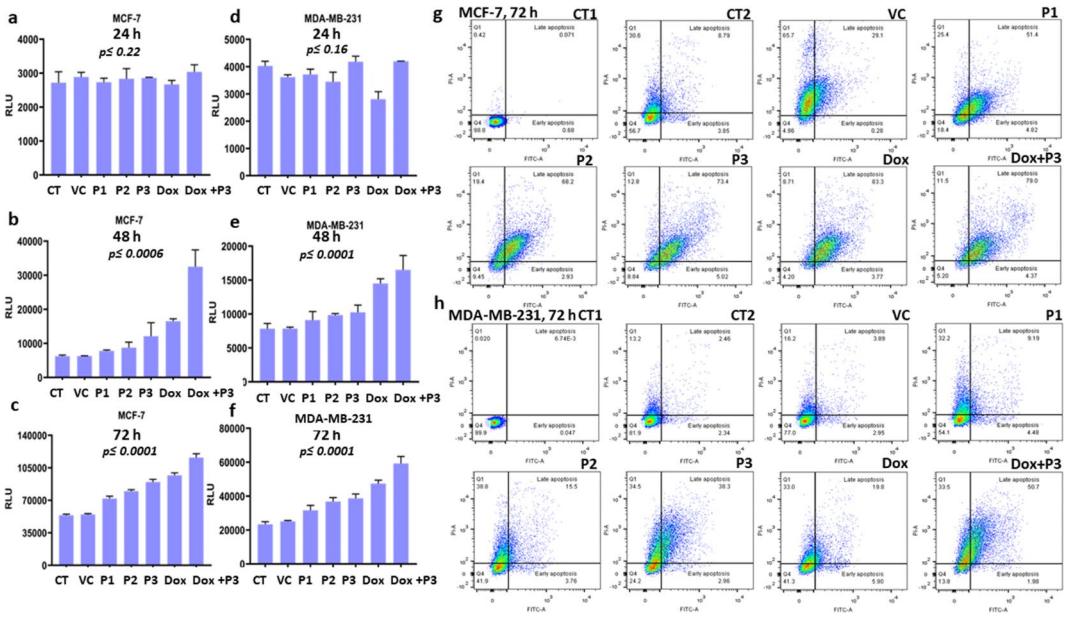

Fig. 3. Assessment of apoptosis by FGDWS induction: Activity of Caspase 3/7 of different treatment group in MCF-7 cell line after (**a**) 24 h, (**b**) 48 h, (**c**) 72 h and in MDA-MB-231 (**d**) 24 h, (**e**) 48 h, (**f**) 72 h. Annexin V and PI assay representing the apoptotic cell population in different treatments groups at 72 h in (**g**) MCF-7 and (**h**) MDA-MB-231 cell lines.

time when cells undergo apoptosis and exposed for binding with Annexin-V, whereas PI stained the necrotic cells by binding with DNA of dead cells.

It has been observed that population of apoptotic cells were increased with increasing FGDWS doses P1 to P3 and in combination of Dox + P3 for both the cell lines. The percent of late apoptotic cell population were highest in Dox + P3 group; 79% in MCF-7 and 50.7% in MDA-MB-231 cell lines (Fig. 3g,h).

Western blot to estimate the expression level of Rac1 and their downstream proteins

Cellular expression level of Rac1 and all other concerned downstream molecules showed changes in treatment group (Fig. 4).

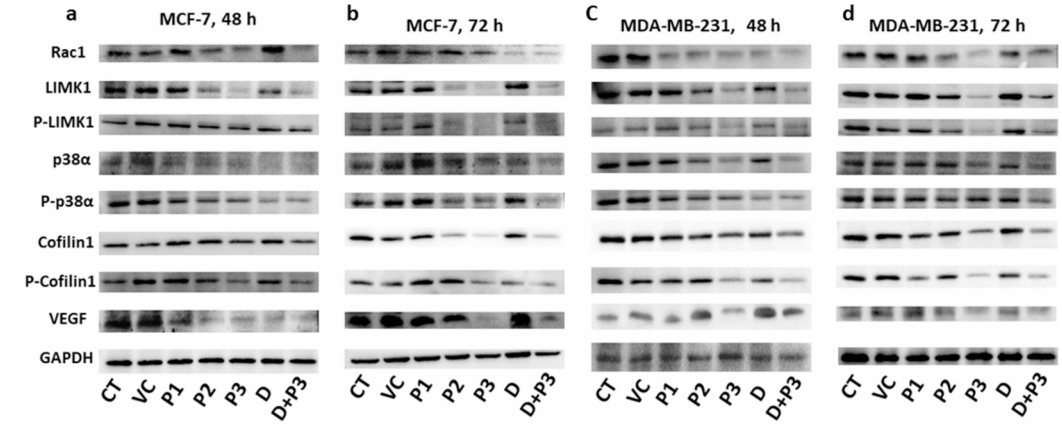

Fig. 4. Western blot represent the expression of downstream pathway of Rac1; p38α, phospho-p38α (Y-182), LIMK1, phospho-LIMK1 (T-508), cofilin1 and phospho-cofilin1 (S-3) in MCF-7 after (**a**) 48 h, (**b**) 72 h and in MDA-MB-231 after (**c**) 48 h, (**d**) 72 h.

The expression of Rac1 in MCF-7 and MDA-MB-231 cell lines were downregulated significantly with increase in concentration of peptide dose from P1 to P3 and highly downregulated in synergy group (Dox + P3) at 48 and 72 h of treatment. Whereas, expression of Rac1 was not affected in treatment with only Dox. For MCF-7 cell line, the percent change in expression level of Rac1 in P1, P2, P3, Dox and Dox + P3 considering CT as control were 1.08, 19.86, 25.84, 13.13 and 32.42, respectively after 48 h, whereas after 72 h of treatments 12.74, 19.41, 31.23, 43.31 and 48.201, respectively. For MDA-MB-231 cell line the percent change of Rac1 after 48 h were 21.41, 28.28, 36.01, 32.57 and 47.13 respectively, after 72 h it were 15.03, 34.94, 48.31, 31.39 and 40.02, respectively. The downstream molecules of Rac1 [p38α, phospho-p38α (Y-182), LIMK1, phospho-LIMK1 (T-508), Cofilin1, phospho-Cofilin1 (S-3)], involved in modulation of cytoskeleton rearrangements and cell movements were also followed the similar downregulated expression pattern like Rac1 after 48 and 72 h of treatments. Their fold change was also estimated as illustrated in Table S1 and S2. VEGF was evaluated to estimate the angiogenic response of cells after treatments. Expression level of VEGF was found to be downregulated after treatments with peptide and Dox. The densitometry analysis of all blots is shown in figure S5 and S6.

Development of tumor mice model

Tumor had appeared on mammary fat pad of swiss albino female mice after 7–8 days of injection of EAC cells and its volume was 15–19 mm^3 (Fig. 5a–d). The tumor growth was progressive, and its volume after 23 days was found to be 125–128 mm^3 (Table 1).

Peptide intervention on tumor progression

The regression of tumor growth was found to be reduced by the treatment of peptide FGDWS alone and in combination with Dox (Fig. 5e). The tumor size was found to be decreased significantly ($p \leq 0.01$) from 125.33 ± 1.69 mm^3 to 52.4 ± 0.86 mm^3 at 45 days after treatments with 300 µm FGDWS peptide and decreased to 40.4 ± 2.53 mm^3 ($p \leq 0.001$) and 31.23 ± 3.10 mm^3 ($p \leq 0.001$) with 600 µm FGDWS and Dox + FGDWS (1 mg/kg + 600 µm), respectively (Fig. 5f–h).

Expression of proteins in serum and tumor tissue of cancer mice model by SPR analysis

Serum level of Rac1, p38α, phospho-p38α (Y-182), LIMK1, phospho-LIMK1 (T-508), Cofilin1 and phospho-Cofilin1 (S-3) proteins were found to be significantly ($p < 0.0001$) higher in serum of TC group compared to HC and after treatment with peptide and Dox (Doses: 300 µm, 600 µm and Dox 1 mg/kg + 600 µm group) the level decreased gradually by SPR analysis as shown in Fig. 5i–o.

Expression level of above-mentioned proteins in the tumor tissue lysate of different experimental group of mice showed similar pattern as shown in serum (Fig. 5p–v). The proteins were downregulated in treatment groups compared to control group in both serum and tumor tissue of mice. The concentration of proteins in serum and tissue was illustrated in (Table 2).

Discussion

Rac1 protein control the multiple signalling pathways that regulate cytoskeleton organization, transcription, and cell proliferation. Rac1 switch over between an inactive GDP-bound state and an active GTP-bound state. Tiam1, a guanine nucleotide exchange factor (GEF) which induced to switch GDP to GTP[8–10]. Rac1 while binding with GDP remain inactive and the moment it switches towards binding with GTP becomes active and bind with downstream effector. It is reported that the 5-LOX/LTC4/CysLT1 signalling pathway regulates EGF-induced cell migration by increasing Tiam1 expression, leading to Rac1 activation and ultimately lamellipodia formation[11] and inhibition of Rac1 induces cell cycle G1/S arrest in cancer cells[12].

In normal condition Rac1 is localised to the cytoplasm in complex with RhoGD1 molecules and block its interaction with downstream effectors. Thus, it plays a critical role in phagocytosis, mesenchymal like migration,

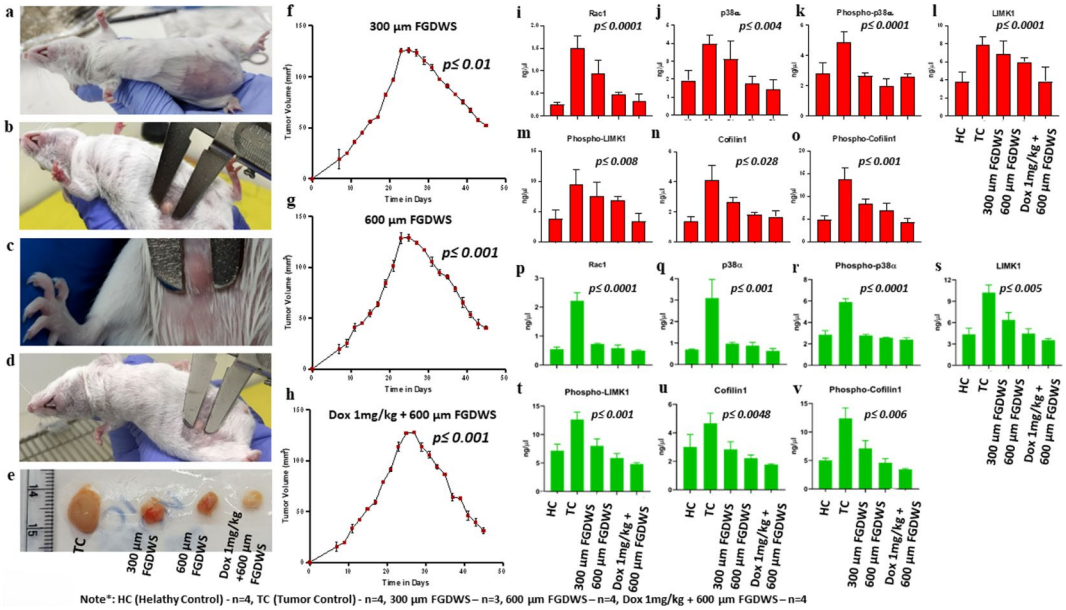

Fig. 5. Assessment of FGDWS on tumor progression: (**a**–**d**) Image of tumor at mammary fat pad of mice at different time points. (**e**) Size of tumor in TC and after treatments with 300 µm FGDWS, 600 µm FGDWS and Dox 1 mg/kg + 600 µm FGDWS. Tumor progression the effect of FGDWS (**f**) 300 µm, (**g**) 600 µm and in synergy with (**h**) Dox. Expression of (**i**) Rac1, (**j**) p38α, (**k**) phospho-p38α (Y-182), (**l**) LIMK1, (**m**) phospho-LIMK1 (T-508), (**n**) Cofilin1, (**o**) phospho-Cofilin1 (S-3) proteins in serum of different experimental groups. Expression of above protein in tissue lysate of different experimental group represent from (**p**–**v**).

Tumor vol.(mm^3) Time (In days)	TC group (mm^3)	300 µm FGDWS (mm^3)	600 µm FGDWS (mm^3)	Dox 1 mg/kg + 600 µm FGDWS (mm^3)
0	0	0	0	0
7	18 ± 2.32	19.16 ± 7.42	19.5 ± 3.93	15.5 ± 4.82
23	126 ± 3.29	125.33 ± 1.69	128.66 ± 3.68	113.66 ± 4.50
Peptide and Dox treatments start point				
45	-	52.4 ± 0.86	40.4 ± 2.53	31.23 ± 3.10
p-value	0.001	0.01	0.001	0.001

Table 1. Tumor growth progression and peptide intervention with time.

S. No.	Protein		HC (Mean ± SD)	TC (Mean ± SD)	300 µm FGDWS (Mean ± SD)	600 µm FGDWS (Mean ± SD)	Dox 1 mg/kg + 600 µm FGDWS (Mean ± SD)	*p*-value
1	Rac1 (ng/µl)	Serum	0.24 ± 0.04	1.51 ± 0.26	0.93 ± 0.28	0.46 ± 0.06	0.32 ± 0.16	0.0001
		Tissue	0.54 ± 0.07	2.21 ± 0.28	0.72 ± 0.02	0.58 ± 0.11	0.63 ± 0.11	0.0001
2	P38α (ng/µl)	Serum	1.92 ± 0.58	3.96 ± 0.52	3.13 ± 0.96	1.77 ± 0.39	1.42 ± 0.55	0.004
		Tissue	0.69 ± 0.02	3.09 ± 0.87	0.97 ± 0.06	0.87 ± 0.15	0.63 ± 0.10	0.001
3	Phospho-p38α (ng/µl)	Serum	2.79 ± 0.71	4.86 ± 0.74	2.66 ± 0.16	1.96 ± 0.46	2.57 ± 0.24	0.0001
		Tissue	2.84 ± 0.39	5.91 ± 0.31	2.77 ± 0.11	2.57 ± 0.03	2.41 ± 0.16	0.0001
4	LIMK1 (ng/µl)	Serum	3.78 ± 1.07	7.83 ± 0.91	6.86 ± 1.46	5.95 ± 0.48	3.82 ± 1.56	0.0001
		Tissue	4.35 ± 0.86	10.21 ± 1.07	6.37 ± 1.04	4.47 ± 0.66	3.55 ± 0.18	0.005
5	Phospho-LIMK1 (ng/µl)	Serum	3.74 ± 1.52	9.53 ± 2.45	7.58 ± 2.25	6.86 ± 0.56	3.41 ± 1.24	0.008
		Tissue	7.17 ± 1.12	12.63 ± 1.29	8.01 ± 1.22	5.86 ± 0.80	4.83 ± 0.22	0.001
6	Cofilin1 (ng/µl)	Serum	1.36 ± 0.29	4.11 ± 0.97	2.68 ± 0.28	1.48 ± 0.14	1.48 ± 0.41	0.028
		Tissue	3.01 ± 0.87	4.66 ± 0.71	2.83 ± 0.53	2.21 ± 0.22	1.76 ± 0.05	0.0048
7	Phospho-Cofilin1 (ng/µl)	Serum	4.87 ± 0.81	13.72 ± 2.46	8.35 ± 1.15	6.84 ± 1.57	4.31 ± 0.78	0.006
		Tissue	5.02 ± 0.39	12.39 ± 1.82	7.14 ± 1.34	4.61 ± 0.69	3.44 ± 0.14	0.001

Table 2. Concentration of proteins in tissue and serum of different experimental group of animal.

axonal growth, adhesion, and differentiation of multiple cell types as well as reactive oxygen species (ROS) mediated cell killing. Rac1 was found to be overexpressed in breast-cancer and expressed more in metastatic breast-cancer compared to non-metastasis[1]. It initiates the cell migration and Li et al. reported targeting Rac1 can effectively reduce the multidrug resistance of breast-cancer cells to neoadjuvant chemotherapy[13]. More than 2 lakhs women diagnosed with breast-cancer in India in the year 2020 and 2.3 million new cases every year all over the world. The number is expected to rise 2.3 lakhs cases in 2025. Between 20 and 30% of early-stage breast-cancer becomes metastasis or stage IV, most aggressive and devastating form of breast-cancer. Metastatic breast-cancer is one of the major causes of death in women globally. Rac1 is the best target for therapeutic agent against breast-cancer as it can be detected as a blood-based biomarker, can differentiate between metastasis and non-metastasis with efficient cut-off value and area under curve[1].

The GEF of Rac1 was first targeted by specific Rac1 inhibitor NSC23766 by interacting with W56 residue in Rac-GEF site. The cavity surrounding W56 of Rac1 was explored and penta peptides were auto docked to design several peptides. Different designed peptides were docked to screen the best peptide which showed strong and stable binding capacity with Rac1. The peptide FGDWS was found to the strongest interacting peptide with Rac1 at the Tiam binding site with the W56 residue. The peptide formed stable H-bonds along with hydrophobic interactions with residues present in the cavity of Rac1 binding site.

The spontaneous activation of Rac1 GDP by various GEF to active Rac1GTP, increases cell proliferation, cell migration, apoptosis, and tumor formation[14–16]. The present study showed the peptide FGDWS inhibits the proliferation of breast-cancer cell line MCF-7; 75% and MDA-MB-231; 60% upto72 h.

The breast-cancer cell lines were treated with very well-known chemotherapy drug, Dox alone and with the combination of peptide FGDWS to investigate the synergetic effect. The peptide-initiated apoptosis in breast-cancer cell line by inducing caspase3/7 expression more in MCF7 and MDA-MB-231 cell lines compared to untreated cell lines and the amount of caspase activity raised was higher in combination of Dox and peptide. The annexin V assay also showed the apoptosis effect of peptide increases with dose dependent manner. The apoptotic cell population of MCF7 cells was 73.6% with higher doses of peptide and 79% in combination with Dox. While in case of MDA-MB-231 cells 38.3% with higher dose of peptide and 50.7% in combination with Dox. It indicates the externalization of membrane phosphatidylserine.

Rac1 is highly expressed in breast-cancer compared to normal breast tissue[17], by activating through epidermal growth factor receptor (EGFR) family. Thereby, many downstream signalling molecules including p21-activated kinases (PAKs), LIMK, PI3K or mitogen-activated protein kinases (MAPKs) provoked by the activation of Rac1[18].

Rac1 is highly expressed in invasive MDA-MB-231 compared to non-invasive MCF-7 breast-cancer cell line. The same result reflected in our study, the basal expression of Rac1 is more enhanced in MDA-MB-231 cells compared to MCF-7 cells. The over expressed Rac1 inhibits vasodilator stimulating phospho protein (VASP) and promote cell migration and invasion in breast-cancer[19]. The peptide FGDWS showed suppression of Rac1 expression in breast-cancer cell line and highly effected with higher doses of peptide and with the combination of Dox, which indicates that the inhibition of Rac1 by FGDWS protect the inhibition of VASP and may prevent the cell migration. It has also been found that the downstream molecules (p38α, LIMK1, Cofilin1) of Rac1 in breast-cancer cell lines also upregulated due to the effect of hyper activation of Rac1. The intervention effect of FGDWS inhibitor treatment showed downregulation of Rac1 and other downstream molecules, which is represented by schematic diagram also (Fig. 6). Rac1 is expressed in both estrogen receptor ER-positive and ER-negative breast-cancer cells. However, ER positive breast-cancer is more sensitive to Rac1 inhibition. Rac1 in breast-cancer is present at the very beginning of the malignant transformation process and stay elevated throughout the metastasis process as indicated by the high expression in the metastasis (17 & 1).

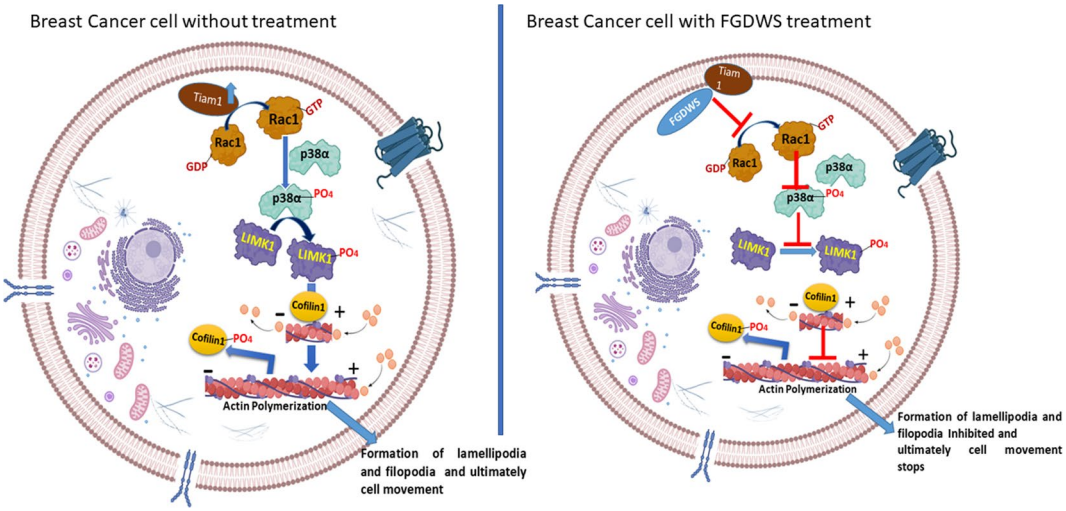

Fig. 6. Schematic diagram represents the breast cancer cell movement mechanism without treatment and alteration in cell movement process with treatment by peptide FGDWS.

Our previous study showed that the Rac1 expression downregulated more in ER positive breast-cancer patients after therapy (Chemo and Radio therapy). In this study inhibition of Rac1 by FGDWS in breast-cancer cell lines downregulated Rac1 as well as other downstream molecules. However, the ER positive MCF7 responded more compared to ER triple negative MDA-MB-231. The expression level of all the proteins were evaluated after the treatment of three different doses of peptide FGDWS and also in combination with Dox peptide to explore the combinatorial effect. Interestingly Cofilin1, the downstream molecule which modulate actin polymerization for lamellipodia and filopodia cycle and crucial for metastasis substantially decreases in both the cell line and much more reduces in ER + MCF-7 cells. The treatment effect of peptide and along with Dox was much more effective than Dox alone. The angiogenesis growth factor; VEGF was also reduced by the effect of inhibitor.

Further, these proteins expression were observed to be highly expressed in the tumor mice model, which downregulated after the intervention of peptide FGDWS and more reduced with the effect of combination of FGDWS and Dox. The intervention of FGDWS also reduced the tumor size of mice. Dox is widely used in cancer therapy, despite its various side effects. Several research are on the line for the combinatorial drug in combination with Dox[20–24].

These in-vitro and in-vivo experiments revealed that peptide FGDWS has potential therapeutic efficiency against breast-cancer targeting Rac1 pathway. This peptide is capable to reduce the tumor size, improve the apoptosis, prevent the cell migration for further metastasis by suppressing the over expression of Rac1 and the downstream molecules by blocking actin polymerization. The combinatorial effect of FGDWS and Dox showed very promising effect on breast-cancer cell line as well as on in-vivo mice model.

Conclusion

It can be concluded from our present and previous study that Rac1 can be a potential specific blood-based biomarker and therapeutic target for metastasis breast-cancer. The peptide FGDWS showed specific therapeutic agent against Rac1 for breast-cancer without developing toxicity on normal cells, hence it holds promising agent for the treatment of breast-cancer. The combinatorial effect of FGDWS and DOX may lead to therapeutic benefits both by enhancing treatment efficacy and by avoiding undesirable side effects.

Methods

Peptide modelling and screening

The crystal structure of the Rac1-Tiam1 complex (Fig. 1a) was analysed to design peptide inhibitors against Rac1[25]. Based on a previously reported inhibitor screening study showed that the small molecule NSC23766 inhibits the interactions between Rac1 and Tiam1 complex[25,26]. The binding pocket is approximately 12 Å x 13 Å with hydrophobic residues W56, V36, L67, A64, and P69 at the bottom and hydrophilic residues K5, D38, N39, D65, R66 along with Y64 at the top of the pocket. We have designed three peptides AVKYM, FGDWS and GFKQC mostly hydrophobic in nature with charged residues Lys and Asp acid at the centre to form salt-bridge interactions with R66 or D365 or D68 of Rac1. The peptides were modelled using Wincoot and energy-minimized and docking was performed using Schrodinger software.

Molecular dynamics simulation

The molecular dynamics simulations of all three peptide-Rac1 complexes were carried out using GROMACS-5.0.7[27,28]. The MD simulations was performed as per protocol described by Malhotra et al.[29]. The complexes were placed in the cubic box of 10 Å from each direction of the protein atoms and the MD was performed with forcefield GROMOS 54a7[30]. The peptide-protein complexes were solvated with the SPC216 water model and neutralized using Na^+ atoms[29–31]. The solvated peptide-Rac1 complexes were energy minimized using the steepest descent algorithm with less than 1000.0 kJ/mol/nm convergent criteria with the subjection of 100 ns molecular dynamic simulation at a constant temperature of 300 K and pressure of 1 atm for 100 ps. The average H-bond occupancy, root mean square deviations (RMSD), root mean square fluctuation (RMSF), Radius of gyration (Rg) and Solvent accessible surface area was calculated for all peptide-Rac1 complexes. The Pymol 2.4.1 was used for visualization and constructing structural Figures[32].

Peptide synthesis

Peptide FGDWS was synthesized following Fmoc and Wang resin chemistry by solid phase peptide synthesis method by automatic synthesizer PS3 (Protein Technology, USA). The solvent used was N, N-Dimethylformamide (DMF), activator were N-Methylmorpholine (NMM), and O-(Benzotriazol-1-yl)-N, N,N′,N′-tetramethyluronium hexafluorophosphate (HBTU). Fmoc group was deblocked by 20% piperidine solution after the synthesis. The peptide was cleaved from Wang resin by trifluoroacetic acid (TFA) followed by peptide precipitation. Peptide was dissolved in 10% acetic acid solution and solidified by lyophilisation process.

Immobilization of Rac1 protein and peptide binding

The binding study of peptide with Rac1 protein was performed by real time label free surface plasmon resonance (SPR) technology by Biacore 3000 instruments (GE Healthcare).

Recombinant purified Rac1 protein was obtained by cloning expression and purification in bacterial expression system following the method described in our previous paper[1]. Rac1 protein was immobilized on CM5 sensor chip by using amine coupling kit. During immobilization process, dextran surface of CM5 sensor chip was activated by applying 1:1 v/v mixture of N-ethyl-N'-3diethylaminopropylcarbodiimide (EDC) (75 µg/µl) and N-hydroxysuccinimide (NHS) (12.5 µg/µl). After surface activation protein in sodium acetate solution (pH 5.0, 10mM) was passed on the flow cell of sensor chip for covalent immobilization and all the activated unreacted surface group were blocked by ethanolamine (pH 8.0). Different concentrations of FGDWS were

passed on immobilized Rac1 and respective RU was obtained. The association (KA) and dissociation (KD) constant were evaluated by fitting the primary sensorgram in BIAevaluation 3.0 software.

Cell culture maintenance

The normal (HEK-293), and breast-cancer (MCF-7 and MDA-MB-231) cell lines were obtained from NCCS, Pune, India and cultured in Dulbecco's modified eagle medium (DMEM) (Gibco Invitrogen, Carlsbad, CA) media, supplemented with 10% fetal bovine serum and 1% penicillin/streptomycin antibiotics. Cells were maintained in humidified environment at 37° C in 5% CO2 supplemented air until confluency was reached 80–90%. All the cell lines used were of passage no 28–33.

Cell viability assay

Toxicity of FGDWS was checked on normal HEK-293 cell line and two breast-cancer cell lines MCF-7 and MDA-MB-231 by 3-(4,5-Dimethylthiazol-2-yl)-2,5-Diphenyltetrazolium Bromide (MTT) assay. HEK-293 was seeded at a density 4×10^3 cells per well in a 96 well plate whereas MCF-7 and MDA-MB-231 cell lines were seeded at a density 5×10^3 cells per well. After overnight adherence, different doses (25 µm, 50 µm, 100 µm, 150 µm, 300 µm and 500 µm for HEK-293 & 50 µm, 100 µm, 200 µm and 350 µm for breast cancer cell lines) of FGDWS were added in their respective well and plates were incubated at 37° C in 5% CO2 incubator for 24 h, 48 h and 72 h. MTT dye (5 mg/ml) was added in each well followed by 4 h of incubation at 37° C in 5% CO2 incubator. Media was aspirated completely from each well and 100 µl/well DMSO was added followed by incubation at 37° C. The absorbance of reaction products was taken at 570 nm using a multiplate ELISA reader (BioRad, USA). The percentage of cell viability was calculated and plotted.

Cell lines experiment group

Seven experimental groups were designed for all the cell line experiments i.e. CT (Control), VC (vehicle control (0.05% Dimethylsulfoxide (DMSO)), three doses of FGDWS (P1: 75 µm, P2: 150 µm, P3: 300 µm), Doxorubicin (Dox: 0.2 µm) and Dox + P3 (0.2 µm + 300 µm).

Cell migration assay

Cell migration assay was performed to assess the rate of cell proliferation and migration. MCF-7 and MDA-MB-231 cell lines were seeded in seven, 35 mm petri dish plate at a density of 0.2×10^6 cells per petri dish. Cells were incubated overnight at 37° C in 5% CO2 incubator for surface adherence. The surface of the petri dish of all experimental group were scratched with the help of sterile 200 µl tip, followed by imaging of all group at zero time. Treatment doses were administered according to treatment group and plates were incubated at 37° C in 5% CO2 incubator for 24 h, 48 h and 72 h. Cell migration was assessed, and image of scratched area was taken after completion of incubation time.

Apoptosis assay

Caspase glow 3/7 assay

Caspase 3/7 assay was performed to check the cellular caspase activity in cell culture medium in different treatment group as described above. MCF-7 and MDA-MB-231cells were seeded at a density of 5×10^3 cells per well in a 96 well plate and incubated for overnight followed by addition of different doses of peptide and Dox for 24 h, 48 h and 72 h. After incubation period, 100 µl of caspase glo 3/7 reagent (substrate/luciferase) (Promega, United States) was added in each well and incubated at 25° C for 30–60 min, to measure the luminescence by luminometer.

Annexin V assay

The percentage of early apoptotic, late apoptotic, necrotic and healthy cell population in different treatments group were investigated by Annexin V-FITC and PI (Propidium iodide) (Thermo Fisher Scientific, United States) staining in flow cytometer (BD Biosciences). MCF-7 and MDA-MB-231 cells were seeded at a density of 0.2×10^6 in 35 mm petri dish and peptide treatment was administered as above. Cells were trypsinized and wash twice with 1x PBS buffer saline. Cells pellet was resuspended in 300 µl 1X binding buffer and 5 µl of annexin V-FITC was added in each group followed by incubation for 10 min. PI (10 µl) was added in each group from 50 µg/ml stock and cells were incubated for 20 min. Cells of each group were passed on flow cytometer and different type of cell population density were recorded in four quadrants Q1, Q2, Q3 and Q4. The data was analysed by using flowJo software.

Western blot to evaluate the expression level of Rac1 and their downstream molecules

Molecular level of Rac1 and their downstream molecules likewise p38α, phospho-p38α (Y-182), LIMK1, phospho-LIMK1 (T-508), Cofilin1 and phospho-Cofilin1 (S-3) were evaluated by Western blot in cell lysate of MCF-7 and MDA-MB-231 with different treatment group after 48 h and 72 h of incubation. Expression of VEGF (vascular endothelial growth factor) was also assessed to check the anti-angiogenic effect of FGDWS. Total cell protein was estimated by bicinchoninic acid assay (BCA) method and bovine serum albumin (BSA) was used as standard. Total of 30 µg protein was run on 10% SDS-PAGE gel for gradual molecular size separation. Protein was transferred from SDS-PAGE gel to PVDF membrane (mdi Membrane Technologies, India) by standard protocol. Non-specific sites of blot were blocked by using 5% non-skimmed milk (Merck Millipore, USA) in TBS-T (10 mM Tris-HCl, 150 mM NaCl and 0.1% tween 20 in miliQ water) for 2 h followed by 3 washing with TBS-T. Blot was incubated with primary antibody rabbit anti human Rac1 IgG (1:250), mouse anti human p38α IgG (1:400), mouse anti human phospho-p38α (Y-182) IgG (1:400), mouse anti human GAPDH IgG (1:500), mouse anti human VEGF IgG (1:300) (Santa Cruz Biotechnology, CA, US), rabbit anti human LIMK1 IgG

(1:500), rabbit anti human phospho-LIMK1 (T-508) IgG (1:500), rabbit anti human Cofilin1 IgG (1:500), rabbit anti human phospho-Cofilin1 (S-3) IgG (1:500), (Immunotag, USA) in 5% BSA TBS-T solution, overnight at 4 °C followed by room temperature incubation for 2 h. Blots were further incubated with HRP (Horse Radish Peroxidase) conjugated secondary antibodies goat anti-rabbit IgG (1:4000) and goat anti-mouse IgG (1:4000) (Rockland, USA). Protein bands were detected by developing membrane in enhanced chemiluminescent system (Pierce ECL Western Blotting Substrate, Thermo Scientific, Rockford, IL) and bands density were analyzed by myImageAnalysis™ software (Thermo Scientific).

Animals

The animal experiments conducted in this study followed protocols approved by the institutional animal ethics committee, AIIMS, New Delhi (154/IAEC-1/2019). All mouse experiments were performed in accordance with the relevant guidelines and regulations by the authors. The authors confirm that the study was conducted in accordance with the ARRIVE guidelines.

The experiment was carried out with 6 weeks old female Swiss Albino mice, obtained from central animal facility, AIIMS. All the mice were acclimatized to standard laboratory conditions including a controlled environment at 25 ± 1 °C and $50 \pm 10\%$ relative humidity with the alternating 12:12-h dark–light cycle and provided with standard food pellets and drinking water ad libitum.

Development of tumor in mice model and peptide intervention

Based on cell line experiments outcomes, 300 µm and 600 µm FGDWS peptide doses were used for in vivo experiments. Mice were grouped into 5 groups i.e. HC (Healthy Control) ($n=4$), TC (Tumor Control) ($n=4$), treatment group: 300 µm FGDWS ($n=3$), 600 µm FGDWS and Dox + FGDWS (1 mg/kg + 600 µm) ($n=4$).

Ehrlich ascites carcinoma (EAC) cell line was used for the tumor development. Cell line was cultured and maintained in peritoneal cavity of mice at a density of 1×10^6 cells. After 7 days, cells were aspirated from peritoneal cavity, pelleted and washed with 1X PBS twice.

The cells density of 3×10^6 were injected at mammary fat pad site of mice. The mice were housed, and tumor growth appeared after 6–8 days of injection. The mice were left till 23 days for tumor growth and from 23rd to 45th day mice with tumor were treated with inhibitors. Tumor size was measured with help of vernier callipers during the experiment.

Estimation of Rac1 and downstream molecules in serum and tissue lysate by SPR

Blood from HC and TC group were collected at 23rd day of experimental time point, whereas blood of treated group mice with peptide and Dox were collected after completion of treatment time point i.e. 45th day. Blood was withdrawn by using standard heart puncture procedure. After blood withdrawal, mice were euthanized by using standard CO2 inhalation method. Mammary fat pad tissue was dissected from all the experimental group. Serum was separated and stored at -80° C. Tissue lysate was prepared by using Radioimmunoprecipitation Assay (RIPA) lysis buffer.

Expression level of Rac1, and downstream molecules were evaluated in serum as well as in tissue lysate by using SPR technology as described in previous paper[1].

Statistical analysis

Statistical analysis was performed by Graphpad prism 9. Descriptive analysis of all variables was carried out, percentage, mean, and standard deviation (SD) were calculated as appropriate. Baseline comparisons between groups was made by using Mann-Whitney test and for more than two groups Kruskal-Wallis test was used. Statistical significance was predefined at a level of $p\text{-value} < 0.05$.

Data availability

All data generated or analyzed during this study are included in this published article and its supplementary information files.

Received: 27 April 2024; Accepted: 4 October 2024
Published online: 23 October 2024

References

1. Singh, A. K. et al. Circulatory level of inflammatory cytoskeleton signaling regime proteins in cancer Invasion and metastasis. *Front. Oncol.* **12**, 851807 (2022).
2. Ridley, A. J. Rho GTPases and actin dynamics in membrane protrusions and vesicle trafficking. *Trends Cell Biol.* **16** (10), 522–529 (2006).
3. Rathinam, R., Berrier, A. & Alahari, S. K. Role of rho GTPases and their regulators in cancer progression. *Front. Biosci.* **16** (1), 2561–2571 (2011).
4. Chen, Q. Y. et al. Silencing of Rac1 modifies lung cancer cell migration, invasion and actin cytoskeleton rearrangements and enhances chemosensitivity to antitumor drugs. *Int. J. Mol. Med.* **28** (5), 769–776 (2011).
5. Su, Z. et al. A novel Rhein derivative: activation of Rac1/NADPH pathway enhances sensitivity of nasopharyngeal carcinoma cells to radiotherapy. *Cell. Signal.* **54**, 35–45 (2019).
6. Dokmanovic, M., Hirsch, D. S., Shen, Y. & Wu, W. J. Rac1 contributes to trastuzumab resistance of breast cancer cells: Rac1 as a potential therapeutic target for the treatment of trastuzumab-resistant breast cancer. *Mol. Cancer Ther.* **8** (6), 1557–1569 (2009).
7. Yoshida, T. et al. Blockade of Rac1 activity induces G1 cell cycle arrest or apoptosis in breast cancer cells through downregulation of cyclin D1, survivin, and X-linked inhibitor of apoptosis protein. *Mol. Cancer Ther.* **9** (6), 1657–1668 (2010).
8. Um, K. et al. Dynamic control of excitatory synapse development by a Rac1 GEF/GAP regulatory complex. *Dev. Cell* **29** (6), 701–715 (2014).

9. Ruihua, H. et al. RhoA regulates resistance to irinotecan by regulating membrane transporter and apoptosis signaling in colorectal cancer. *Oncotarget* **7** (52), 87136 (2016).
10. Cardama, G. A., González, N., Maggio, J., Menna, P. L. & Gomez, D. E. Rho GTPases as therapeutic targets in cancer. *Int. J. Oncol.* **51** (4), 1025–1034 (2017).
11. Magi, S. et al. 5-Lipoxygenase and cysteinyl leukotriene receptor 1 regulate epidermal growth factor-induced cell migration through T iam1 upregulation and R ac1 activation. *Cancer Sci.* **105** (3), 290–296 (2014).
12. Linna Liu, H. et al. Inhibition of Rac1 activity induces G1/S phase arrest through the GSK3/cyclin D1 pathway in human cancer cells. *Oncol. Rep.* **32**, 1395–1400 (2014).
13. Li, Q. et al. Rac1 activates non-oxidative pentose phosphate pathway to induce chemoresistance of breast cancer. *Nat. Commun.* **11** (1), 1456 (2020).
14. Payapilly, A. & Malliri, A. Compartmentalisation of RAC1 signalling. *Curr. Opin. Cell Biol.* **54**, 50–56 (2018).
15. Kazanietz, M. G. & Caloca, M. J. The rac GTPase in cancer: from old concepts to new paradigms. *Cancer Res.* **77** (20), 5445–5451 (2017).
16. Maldonado, M. D. & Dharmawardhane, S. Targeting rac and Cdc42 GTPases in cancer. *Cancer Res.* **78** (12), 3101–3111 (2018).
17. Schnelzer, A. et al. Rac1 in human breast cancer: overexpression, mutation analysis, and characterization of a new isoform, Rac1b. *Oncogene* **19** (26), 3013–3020 (2000).
18. Nagase, M. & Fujita, T. Role of Rac1–mineralocorticoid-receptor signalling in renal and cardiac disease. *Nat. Rev. Nephrol.* **9** (2), 86–98 (2013).
19. Han, G. et al. Positive regulation of migration and invasion by vasodilator-stimulated phosphoprotein via Rac1 pathway in human breast cancer cells. *Oncol. Rep.* **20** (4), 929–939 (2008).
20. Elfadadny, A. et al. Natural bioactive compounds-doxorubicin combinations targeting topoisomerase II-alpha: anticancer efficacy and safety. *Toxicol. Appl. Pharmcol.* **27**, 116405 (2023 Jan).
21. Qiu, C. et al. Advanced strategies for nucleic acids and small-molecular drugs in combined anticancer therapy. *Int. J. Biol. Sci.* **19** (3), 789 (2023).
22. de Padua, T. C. et al. A systematic review of published clinical trials in the systemic treatment of adrenocortical carcinoma: An initiative led on behalf of the Global Society of Rare Genitourinary Tumors. Clinical Genitourinary Cancer. (2022).
23. Chen, Y., Xu, H., Shan, N. & Qu, H. Pegylated liposomal doxorubicin (PLD)-containing regimen as a novel treatment of monomorphic epithelial intestinal T-cell lymphoma (MEITL): a case report and review of literature. *Medicine* **101** (44). (2022).
24. Younes, M. et al. The synergistic effects of curcumin and chemotherapeutic drugs in inhibiting metastatic, invasive and proliferative pathways. *Plants* **11** (16), 2137 (2022).
25. Gao, Y., Dickerson, J. B., Guo, F., Zheng, J. & Zheng, Y. Rational design and characterization of a Rac GTPase-specific small molecule inhibitor. Proceedings of the National Academy of Sciences. 101 (20) 7618-23. (2004).
26. Zheng, C. et al. Computational prediction of hot spots and binding site of inhibitor NSC23766 on Rac1 binding with Tiam1. *Front. Chem.* **8**, 625437 (2021).
27. Abraham, M. J. et al. GROMACS: high performance molecular simulations through multi-level parallelism from laptops to supercomputers. *SoftwareX* **1**, 19–25 (2015).
28. Berendsen, H. J., van der Spoel, D. & van Drunen, R. GROMACS: a message-passing parallel molecular dynamics implementation. *Comput. Phys. Commun.* **91** (1–3), 43–56 (1995).
29. Malhotra, L. et al. Curcumin rescue p53Y220C in BxPC-3 pancreatic adenocarcinomas cell line: evidence-based on computational, biophysical, and in vivo studies. *Biochim. et Biophys. Acta (BBA) Gen. Subj.* **1865** (2), 129807 (2021).
30. Schmid, N. et al. Definition and testing of the GROMOS force-field versions 54A7 and 54B7. *Eur. Biophys. J.* **40**, 843–856 (2011).
31. Mark, P. & Nilsson, L. Structure and dynamics of the TIP3P, SPC, and SPC/E water models at 298 K. *J. Phys. Chem. A* **105** (43), 9954–9960 (2001).
32. Seeliger, D. & de Groot, B. L. Ligand docking and binding site analysis with PyMOL and Autodock/Vina. *J. Comput. Aided Mol. Des.* **24** (5), 417–422 (2010).

Acknowledgements

Authors acknowledged Indian Council of Medical Research for providing the fellowship to Abhinay Kumar Singh.

Author contributions

AKS: Methodology, Data curation, Validation. Writing. TK & EAS: Software. DV & AS: Validation. AB: Conceptualization, SD: Conceptualization, supervision, verification, writing original draft preparation Reviewing and Editing,

Declarations

Competing interests

The authors declare no competing interests.

Additional information

Supplementary Information The online version contains supplementary material available at https://doi.org/10.1038/s41598-024-75351-y.

Correspondence and requests for materials should be addressed to S.D.